The United Nations University

GEOTHERMAL TRAINING PROGRAMME
Orkustofnun, Grensásvegur 9,
IS-108 Reykjavík, Iceland

Reports 1997
Number 5

GEOCHEMICAL INTERPRETATION OF THERMAL FLUID FROM THE YANGYI HIGH-TEMPERATURE FIELD, TIBET, CHINA

Du Shaoping
Geothermal Geology Team,
Bureau of Geology and Mineral Resources of Tibet,
Jin Zhu Road 15,
Lhasa, Tibet,
P. R. CHINA

ABSTRACT

Aquifer temperatures of 12 geothermal wells in the Yangyi field whose measured reservoir temperatures range from 104 to 207°C have been estimated from the chemical composition of the discharged fluid. Subsurface temperatures calculated using silica geothermometers are in agreement within a 10°C range compared to measured temperature, while large differences have been obtained for cation geothermometers due to mixing with cold water, chemical reactions in the upflow, lack of equilibration in the reservoir or because some of the temperature functions used are not applicable. Most of the minerals studied have apparently not equilibrated with the solution in the reservoir.

Three types of mixing models have been applied to evaluate the temperature of the hot water component in the geothermal reservoir, the chloride-enthalpy model, the silica-carbonate model and the warm spring silica-enthalpy model. The three models indicate subsurface temperatures of 188-253°C which are similar to those found after drilling.

1. INTRODUCTION

The Yangyi geothermal field is one of the high-temperature geothermal fields in Tibet. It is located in the southern part of the Nagqu-Ngemo geothermal active belt, 45 km southwest of Yangbajing and 75 km southeast of Lhasa, the capital city. Investigations carried out since 1981 include geological studies, geophysical surveys, geochemical exploration and completion tests on wells. Geothermal resource evaluation was completed in 1990, with 30 MW of power potential being estimated which suggests that Yangyi is the second largest high-temperature geothermal field in Tibet.

Geochemistry has been used quite extensively since the seventies as a tool of exploration for geothermal resources and for the subsequent development and exploration of these resources. The application of geochemistry in exploration surveys emphasizes the prediction of subsurface temperature and the identification of the recharge areas. Interpretation of thermal fluid composition will give a better

understanding of the origin of the fluid and the chemical processes that take place during its transport.

A sampling programme including collection of local cold water, hot spring water and well discharges was in operation from 1981 to 1989. Twenty-seven samples (Figure 1) have been chosen for this study which focuses on geochemical interpretation of chemical data on cold water, hot spring water and well discharges. Calculation of reservoir temperature using various geothermometers was carried out. Solution-mineral equilibria and mixing models have been used in an effort to understand the physical processes which take place in the geothermal system. A good agreement is obtained for the estimated reservoir temperature using different methods, including the logging of drilled wells.

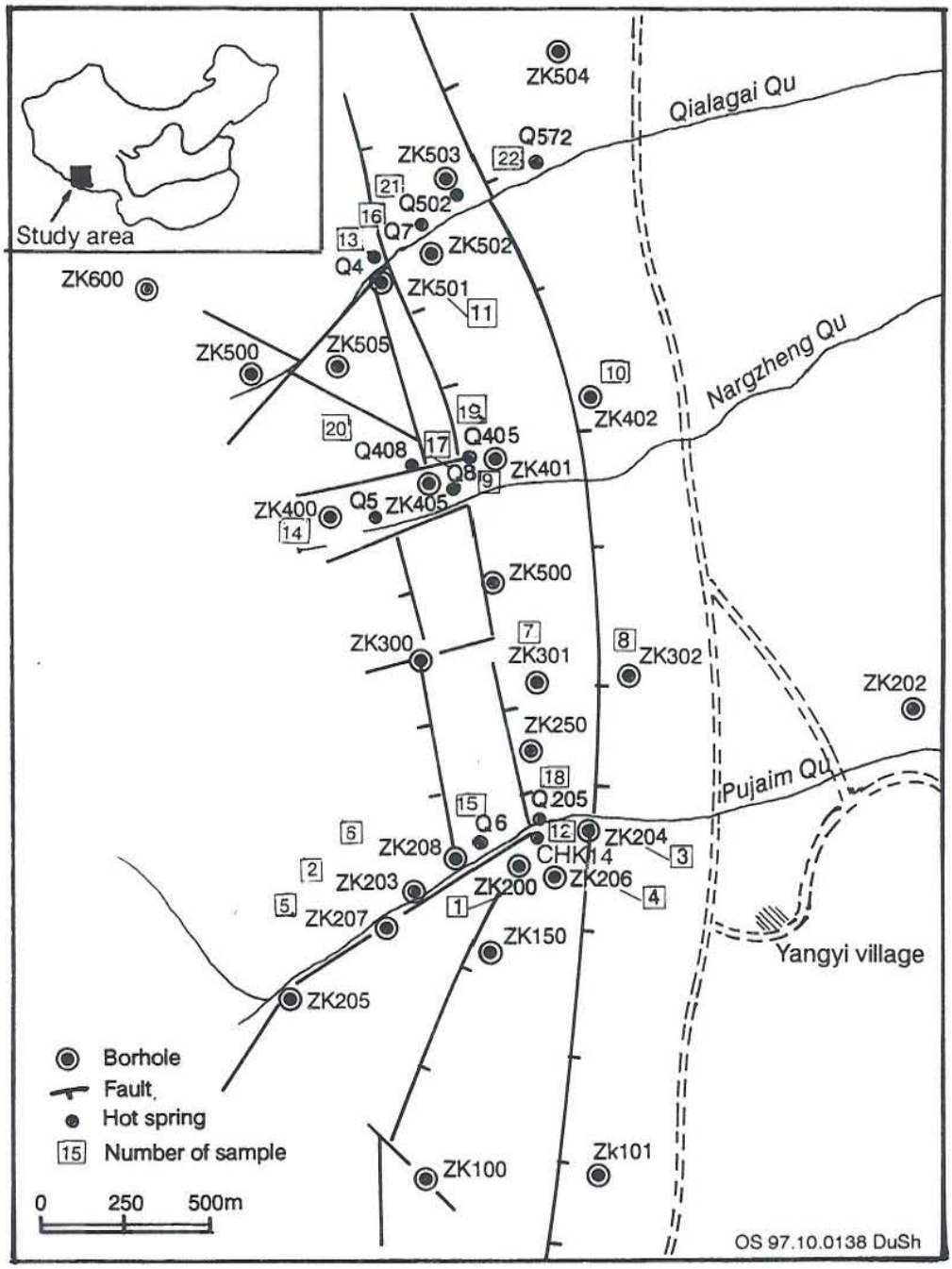

FIGURE 1: The Yangyi geothermal field and location of sampling sites (modified after Qin, 1996)

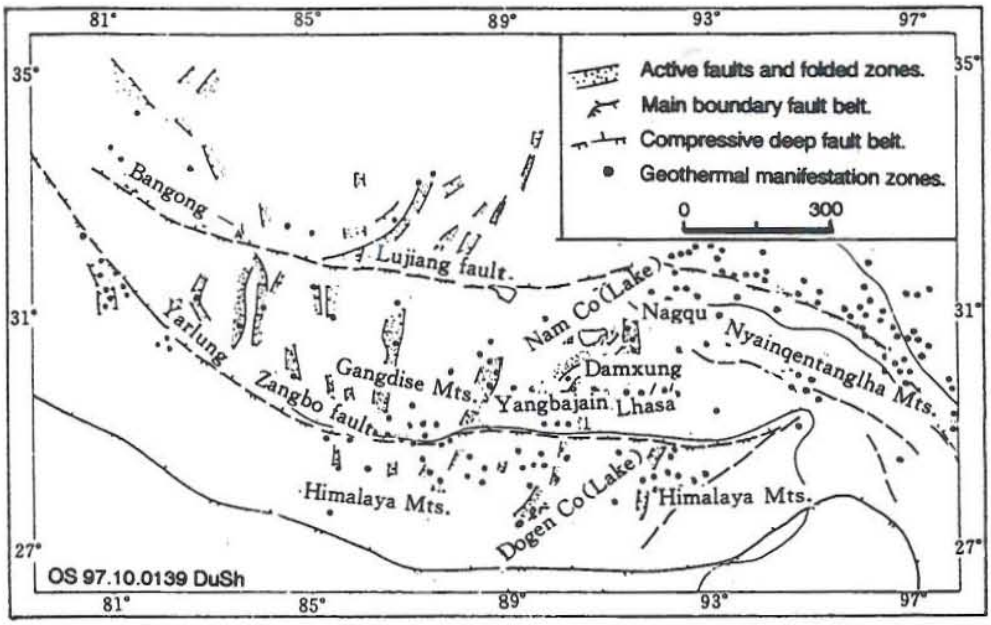

FIGURE 2: Geothermal manifestations and main tectonic features in Tibet (modified from Qin, 1996)

2. GEOLOGICAL SETTING AND SURFACE MANIFESTATIONS

The Tibetan plateau was created by subduction of the Indian and Eurasian constructive plates and overall lift since the end of the Cretaceous. These collisions produced many great fundamental structure zones with E-W strike. Due to the collision of plates, scores of active tectonic zones trending N-S, NE-SW and NW-SE have formed since the Tertiary (Figure 2). These active tectonic zones are characterized by earthquakes and extensive hydrothermal activity. The Golug-Yangbajing-Nyemo geothermal active belt is one of them (Figure 3).

2.1 Geological setting

The Yangyi geothermal field is one of the main geothermal fields on the Golug-Yangbajing-Nyemo geothermal active belt with an elevation of 4600-4800 m a.s.l. The geothermal field is distributed to the west of the N-S trending Yangyi faulted basin. It is linked with Getaguo basin to the north. East and west of the basin are the southern parts of the Nyanqentanglha Mountains and the Tanglha Mountains

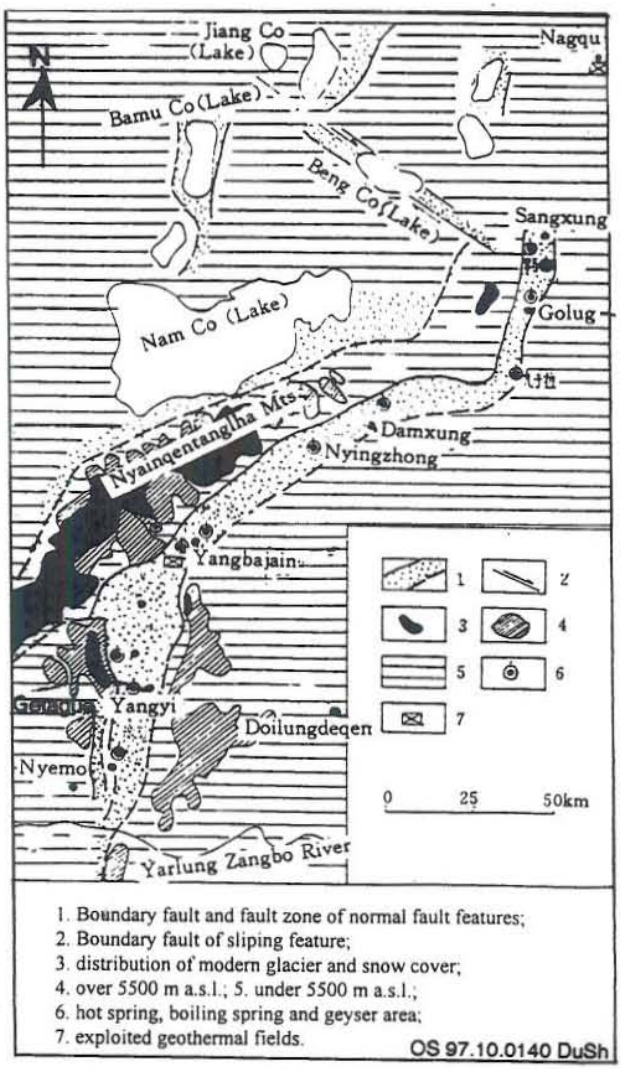

FIGURE 3: Belt of geothermal activity in the Gulug-Yangbajing-Nyemo zone (mod. Qin, 1996)

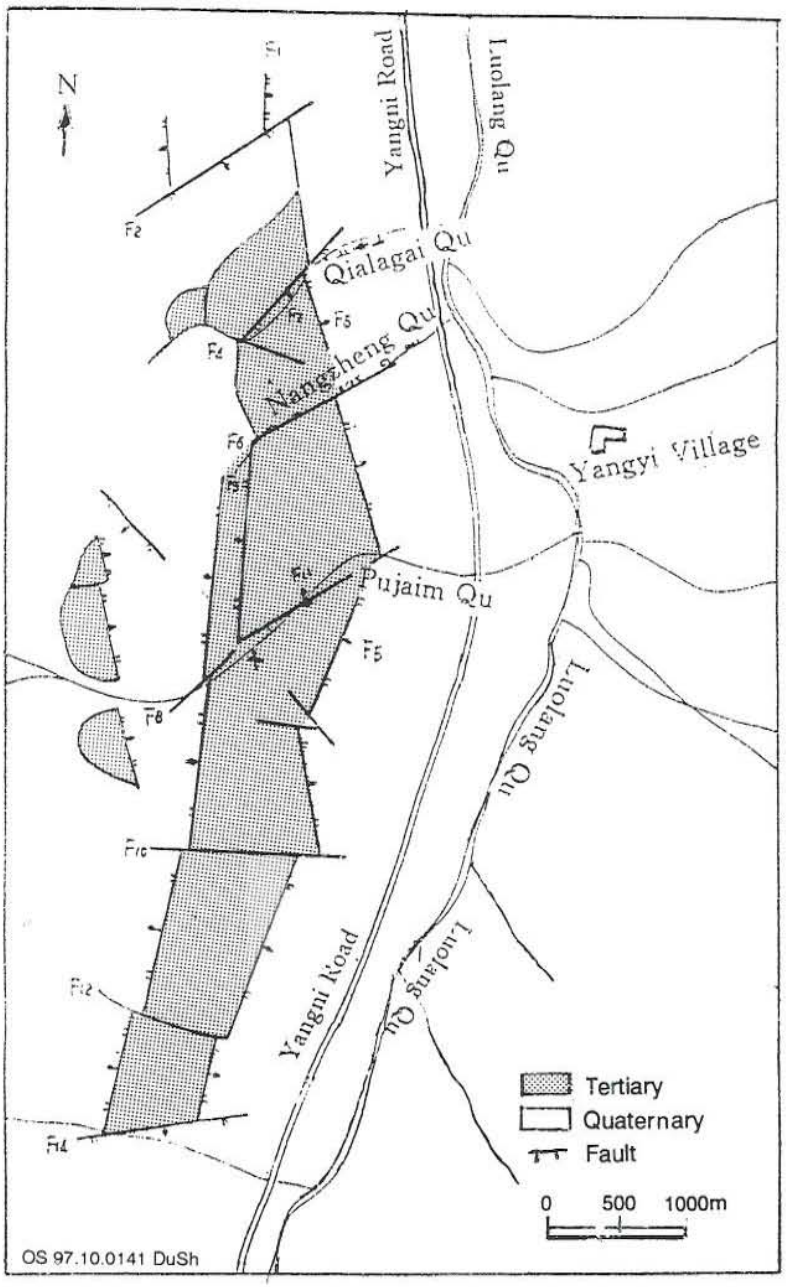

FIGURE 4: Geologic structures of the Yangyi geothermal field (modified from (Qin 1996)

respectively. The Luolangqu river extends from south to north and the hills on each side are over 5000 m a.s.l.

The surface rock outcrops in the Yangyi field are composed of Tertiary volcanics and Quaternary deposits. The major volcanic rocks are andesite and trachytes and the Quaternary deposits are mostly glacial accumulation about 600 m thick in the basin (Qin, 1996).

Magmatic activity was intense in the Himalayan period and the lithology is variable as shown by the eruptive porphyritic granite, and granite intruding into Cretaceous and Tertiary formations. Isotope dating suggests an age of 11-67 m.y. The eruptive rocks may be from two periods: the andesite and trachytes from Eocene and Oligocene with isotope dating suggesting an age of 32-45 m.y., and the andesite and ignimbrites from Miocene and Pliocene with isotope dating suggesting an age of 9 m.y. (Qin, 1996).

The Yangyi geothermal field is controlled by a crisscross of fault systems (Figure 4). The systems consist of several faults trending N-S and NE-SW. The N-S active faults are intersected by a series of NE-SW secondary faults in the field, forming horst block structures (Qin, 1996).

2.2 Surface manifestations

The hydrothermal activity is concentrated in the three valleys of Qialagai, Nangzhen and Pujaimqu from north to south. Surface manifestations in the three valleys are dominated by springs and spring clusters with temperatures ranging from 40 to 85°C and sinter over a large area (Qin, 1996).

The convergence of faults forms a large scale fractured zone, over 100 m wide in Qialagai valley. Due to thin cap rock and well-developed fractures, the hydrothermal activity is the greatest and the

manifestation intensity highest in this valley. Numerous steaming pits or holes with temperatures up to 90°C sit on the south side of the valley (Qin, 1996). A group of boiling springs with temperatures exceeding 80°C are situated in an area 400 m long and 100 m wide. In addition, steaming pools and hot water ponds lie on the sinter which extends about 1500 m to the northeast (Figure 5).

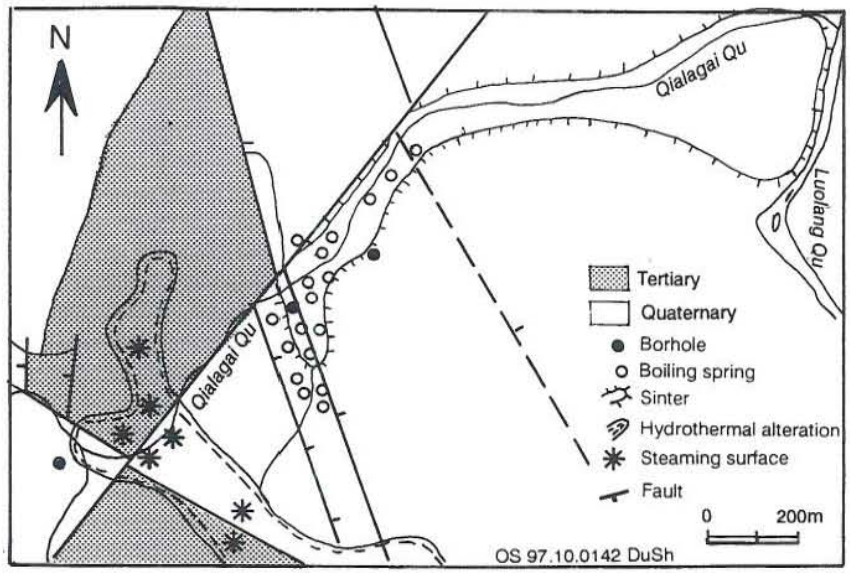

FIGURE 5: Geothermal activity along the Qialagai Qu river (modified from Qin, 1996)

The Pujaim hydrothermal area is situated south of the Yangyi geothermal field, with a NE-SW trending fault, F11 (Figure 6) on the southern slope which intersects the N-S trending fault belt, has a northerly direction dip and forms a valley 50 m wide and 1500 m long. Hydrothermal activity is intense in this valley. In the early period, a number of springs appeared on the 350 m long and 150 m wide sinter fan. The platform exposed by the borehole is 30 m thick, overlying andesite. On the ancient sinter deposits, a small spring remains in the centre with thermal water overflowing from the sinter platform. With sustained erosion, a 2 m wide and 3 m deep ditch formed and a mixture of hot water and streams formed a waterfall here. There are four boiling springs and a gushing spring of temperature 86°C on the sinter platform. The sinter depositis is nearly 5 m in height at the surface and shows the configuration of neotectonic movement (Qin, 1996).

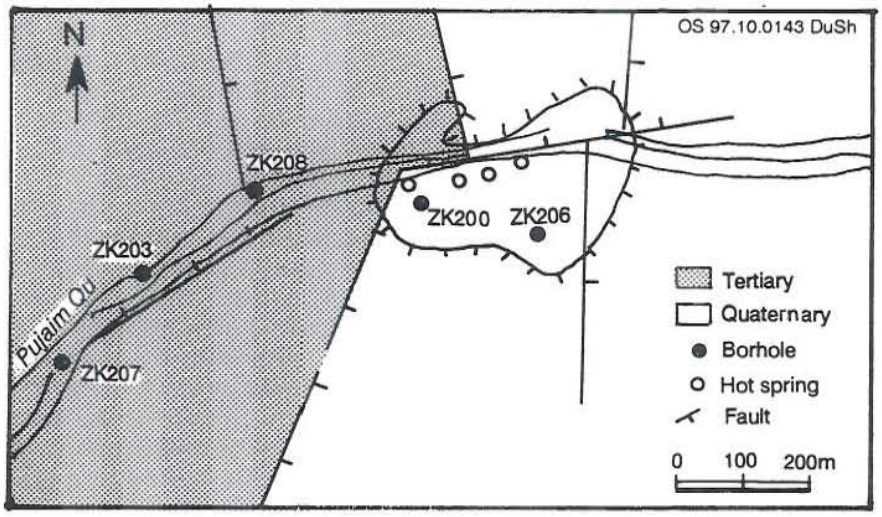

FIGURE 6: Geothermal activity along the Pujaim Qu river (modified from Qin, 1996)

Hydrothermal alteration is intense in the Yangyi field. For example, granite-porphyry and clastic rocks have been altered by the upwelling of fluid along fractures. Hydrothermal minerals identified in the Yangyi field are dominated by clay minerals, silica and carbonate. On the surface, alunite, chalcedony and α- cristobalite occur in the centre of acid fracture zones, trending towards less acidic conditions with an assemblage of kaolinite, montmorillonite, α-cristobalite and opal occurring far from the fracture (Zhu and Xu, 1992).

3. REVIEW OF GEOTHERMAL EXPLORATION

Exploration of the Yangyi geothermal field began in the 1970s. A reconnaissance survey, detailed survey and prospecting started in the early 80s. A geothermal resource evaluation was completed in 1990; subsequently, the geothermal reservoir was certified by the State Reserve Commission

3.1 Geophysical exploration

Geophysical surveys were carried out from 1981 to 1989, including a gravity survey, magnetic measurements and resistivity measurements. As hydrothermal activity is commonly associated with fractures in the Yangyi field, magnetic mapping and the gravity survey were performed to locate faults. Results of magnetic measurements show that faults trending N-S and NE-SW are probably tilted to the east and southeast, respectively.

The thermal anomaly (which is located in the centre of the field) is about 15.6 km^2 and 5.2 km^2, as delineated, respectively, by the 10 Ωm and 5 Ωm resistivity contours (Liang, 1992).

3.2 Drilling history

Much of the exploration of the field was carried out between 1986 and 1990. Forty-seven boreholes have been drilled with a total depth of about 5400 m, the deepest borehole being 1100 m and the shallowest 20 m (Qin, 1996).

Based on the results of the resistivity measurements, the first three wells (ZK200, ZK301 and ZK501) were drilled in the eastern part of the field. Discharge was measured at the end of drilling. ZK200 yielded 2.6 l/s and its maximum downhole temperature was 172°C, but with increasing depth temperature decreased significantly below the maximum point (Liang, 1992). ZK203 and ZK401 were drilled in 1987. A considerable amount of water was encountered in ZK203 whose total flowrate was 65 l/s the maximum downhole temperature was 203°C (Liang, 1992). Between 1988 and 1990, some wells were drilled to the west of fracture F5. The highest temperature, about 207°C, was observed ZK208 in the southern part of the field. Its mass flowrate was about 110 l/s and, thus, its power potential was estimated at about 10MW (Liang et al.,1990).

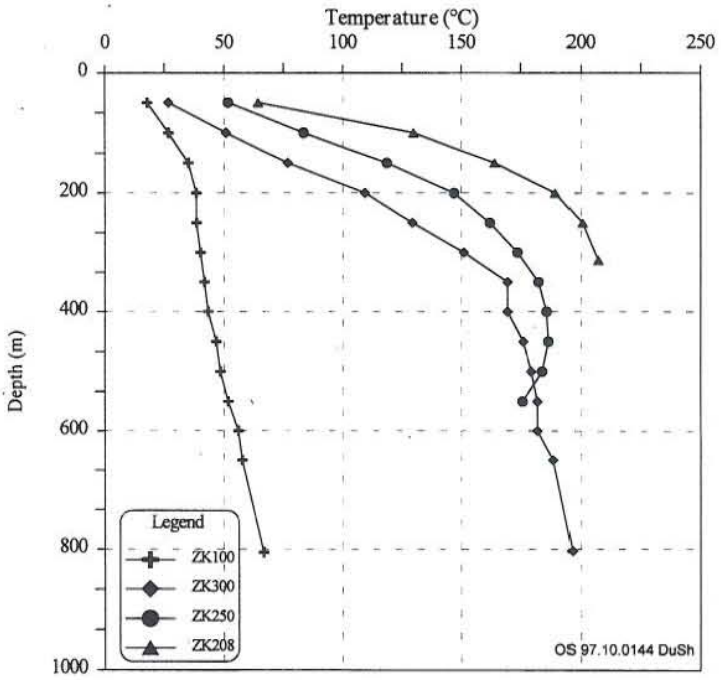

FIGURE 7: Temperature profiles for wells in the Yangyi field

Results of temperature measurements indicate that most of the aquifers are located below about 320 m depth (Figure 7); the thermal gradient was up to 67°C/100m in the uppermost 300 m (Liang et al., 1990).

4. CHEMICAL CHARACTERISTICS OF THE THERMAL FLUIDS

The composition of geothermal fluids depends on many factors. The most important are temperature dependent reactions between host rock and water. Leaching plays an important role when the amount of a particular constituent is too small to attain equilibrium. However, processes of mixing, boiling and cooling usually have a significant influence on the final composition of the geothermal water.

The present geochemical study is based on 27 samples selected from wells, hot springs and local cold water. All the samples were collected in the year 1989, and analyses were performed in the chemical laboratory of the Geothermal Geological Team of Tibet. Ionic balance was calculated from the chemical data using the program WATCH (Arnórsson et al., 1982; Bjarnason, 1994). The chemical composition of all samples is shown in Table 1. The first twelve samples are from wells, samples 13 to 22 are from hot springs and the last five samples represent local cold water.

Sulphate concentrations are relatively large in samples from wells and some hot springs but in all geothermal samples as well as in the local cold water carbonate (represented by total carbonate as CO_2) is the major anion. Sodium is the dominant cation in all samples of thermal water, but in the cold water the calcium concentration is higher than the sodium concentration. The pH ranges from 5.69 (sample 17) to 9.68 (sample 19). The Al concentration was determined in sample 20 only. The stable isotope ratios of the thermal water, both from wells and springs, are close to those of the local cold water.

The gas composition of sample 1 is CO_2-23.67%, N_2-60.65%, H_2-0.37% He-0.475 and O_2-13.72% (by volume). The sample was analysed in the Institute of Geological Exploration and Development in Shichang Province.

4.1 Isotope data for the thermal water

The isotopic analyses of water samples from springs and wells give information on the origin of the field discharges, on their age, on possible underground mixing between different waters, on water-rock interaction, and on steam separation processes. It is suggested that a sample of groundwater discharging from either a cold or hot spring, with a deuterium value similar to the mean value of the local precipitation can indicate a local origin of the groundwater (Árnason, 1976).

Figure 8 shows that all the data on local cold water, hot springs and discharges from wells indicate relationships between δD and $\delta^{18}O$. All the data points for local cold water plot approximately on the world meteoric line. The deuterium ratio of the spring water is about -160‰, which is similar to that of local cold water sample 25, which was sampled from a high mountain area southwest of the Yangyi field. This is probably

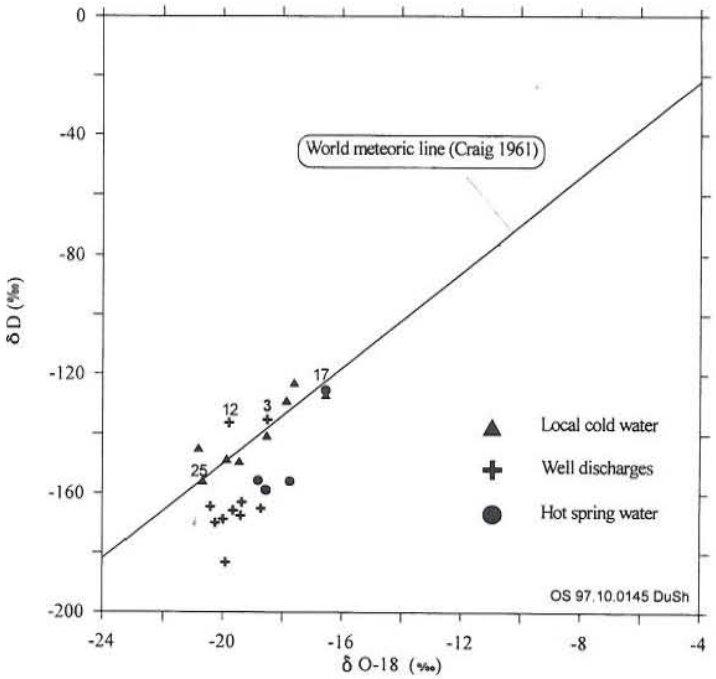

FIGURE 8: δD vs. $\delta^{18}O$ for the Yangyi waters

TABLE 1: Chemical composition of thermal waters and cold waters from Yangyi (ppm)

No.	Source	T(°C)	pH	CO_2	B	SiO_2	Na	K	Mg	Ca	F	Cl	SO_4	Fe	Li	Al	δ D	$\delta^{18}O$	TDS	Ionic bal.
	Well																			% diff.
1	ZK200	70	7.59	493.01	19.678	297	430	32	1.1	16.45	13.79	159	205	0.5	6.5		-161.25	-18.01	1512.41	1.41
2	ZK203	61	7.97	463.96	18.67	285.2	394	28.7	0.09	25	15.88	160.8	210	1.96	6.2		-164.35	-19.22	1448.44	-5.44
3	ZK204	72	8.22	719.82	18.67	209.4	560	32	0.22	16.3	15.12	194.6	230	0.18	5		-132.9	-18.08	1802.32	-6.12
4	ZK206	21	7.2	690.8	18.92	210	460	30		16.6	12.92	166.6	200	0.9	6.9		-166	-19.48	1547.47	-7.65
5	ZK207	83	8.1	599.2	29.75	231	464	7	2.6	12.95	11.5	171.6	188		12.24		-161.1	-19.79	1568.22	-8.59
6	ZK208	86	8.49	461.03	33.02	473	422	42	6.23	1.16	18.24	180.6	172		16.1				1704.96	-5.01
7	ZK301	79	8.58	480.93	14.38	302.5	424	38.2	1.1	10.87	18.24	177.2	200	0.06	9.8		-164.05	-18.76	1555.39	-8.18
8	ZK302	77	7.76	615.47	19.42	174	452	24	0.75	15.94	9.5	158	205	0.28	4.8		-181.68	-19.62	1480.61	-7.71
9	ZK401	79	8.54	507.65	15.99	192.5	452	30	0.88	18.12	12.08	160.3	165		6.9		-163.8	-19.31	1431.18	3.25
10	ZK402	65	8.86	517.43	17.48	126.5	476	9.1	0.92	14.11	9	150.4	235	0.52	6.2				1435.34	-3.8
11	ZK501	77	8.1	453.69	16.15	297	404	28.6	0.31	7.25	22.04	173.4	205	0.2	10		-160.8	-18.97	1467.96	-10.28
12	CHK4	34	8.35	314.96	7.06	152	188	17.3	9.89	43.62	5.02	80.91	105	0.4	4.8		-134.65	-19.5	841.92	-4.12
	Spring																			
13	Q4	86	9.4	256.59	29.895	166	434.5	24.8	1.13		20.52	181.6	36		14.95		-158.8	-18.57	1521.1	21.19
14	Q5	83	9	274.35	28.419	144	384	19.6	0.64	0.81	18.24	167.9	250		14.55		-158.97	-18.55	1299.2	-7.96
15	Q6	84	8.86	240.63	13.472	164	145	10	7.12	23.88	4.37	68.51	74		4.6		-155.6	-18.82	673.1	-18.68
16	Q7	57	8.7	409.93	30.374	144	480.5	480.5	0.74	0.81	19.76	188.4	160		22.05		-155.9	-17.75	1301.3	49.91
17	Q8	78	5.69	16.46	4.54	168	5.5	5.57	0.39	2.83	0.29	4.45	20				-125.36	-16.56	216.5	-10.49
18	Q206	77	8.01	313.81	6.81	170	206	16.88	8.66	32.24	15.12	77.06	100		4.8				852.92	-3.77
19	Q405	74	9.68	236.36	20.43	198	400	24.6		1.81	19.3	161.2	255		10.8				1358.7	-11.01
20	Q408	82	6.2	19.21	2.31	165.3	7.64	7.06	0.49	3.85	0.67	3.55	18	0.39	0	0.032			219.22	11.18
21	Q502	50	8.5	336.01	25.85	146.7	362.9	12.2		4.81	24.7	151.7	84		11.52				1195.6	5.2
22	Q572	50	7.6	80	13.43	80	180.2	8.45	0.34	16.43	8.36	83.19	44		5.01				624	48.2
23	Q2	5	7.29	45.15	1.219	19.6	2.62	0.54	2.7	13.76	0.067	1.03	3				-149.21	-19.45	73.7	2.78
24	River	13	7.3	36.99	1.22	18.8	4.5	1.18	2.36	10.53	0.15	1.71	12				-140.5	-18.53	75.9	-11.18
25	River	14	7.43	26.35	1.59	15.6	2.81	0.94	1.96	7.93	0.16	1.71	2				-155.7	-20.68	51.5	7.93
26	River	6.5	7.49	26.48	1.11	7.4	1.82	1.82	1.47	8.1	0.04	12.01	1.03		0.62		-144.7	-20.82	38.9	-23.25
27	River	7	7.97	40.68	1.48	12.4	3.48	3.48	2.11	13.36	0.046	20.19	1.71		1.14		-148.4	-19.88	63	-34.1

the recharge area for the hot springs. Horizontal oxygen shift observed for most of the hot springs might be controlled by oxygen isotope exchange with minerals forming the rock matrix. Sample 17 plotted close to the meteoric line, suggesting that this water is recharged by local precipitation.

The isotope ratios for well discharges show a significant variation in δD, between -161.1‰ and 181.68‰. The recharge area for this water is probably located in the higher mountain area, further southwest than the spring waters. Giggenbach (1992) suggested that rather than being due to water-rock isotope exchange within the crust, ^{18}O shift may largely reflect varying degrees of additional mixing with D in ^{18}O-enriched "andesitic" waters, which could be an alternative explanation for the isotope ratios observed in the Yangyi geothermal water.

Sample 3 plotted close to the meteoric line, and seems to originate from local cold water. Sample 12 shows a negative isotope shift, suggesting that this water is probably formed by steam heating of local cold water.

4.2 Relative Cl, Li and B contents

The Cl-Li-B triangular plot has been suggested to trace the origin of the thermal fluid. Of the three components, Li is probably least affected by secondary processes. Therefore, it may be used as a "tracer" for the initial deep rock dissolution process and as a reference for evaluating the possible origin of the other two important "conservative" constituents of thermal waters, Cl and B (Giggenbach,1991). Once added, Li remains largely in solution. Both Cl and B are added to the Li containing solutions in proportions close to those in crustal rocks. At high temperatures Cl occurs largely as HCl, and B as H_3BO_3. Both are volatile and easily mobilized by high-temperature steam. They are, therefore, quite likely to have been introduced with the magmatic vapours which lead to the formation of the deep acid brine responsible for rock dissolution. At low temperature, the acidity of HCl increases rapidly, and it is soon converted by the rock to the less volatile NaCl; B remains in its volatile form to be carried in the vapour phase even at quite low temperatures.

With the exception of cold water, the chloride concentration of Yangyi water is not significantly different in discharges from wells and springs. The Cl/B mass ratios for all the samples are in a range of 5.87-12.33 (Table 2), indicating the origin of chloride and boron to be mainly dissolution from host rocks.

A plot of relative chloride, lithium and boron concentrations (Figure 9) shows that the thermal fluid may have originated from reaction with local altered rocks.

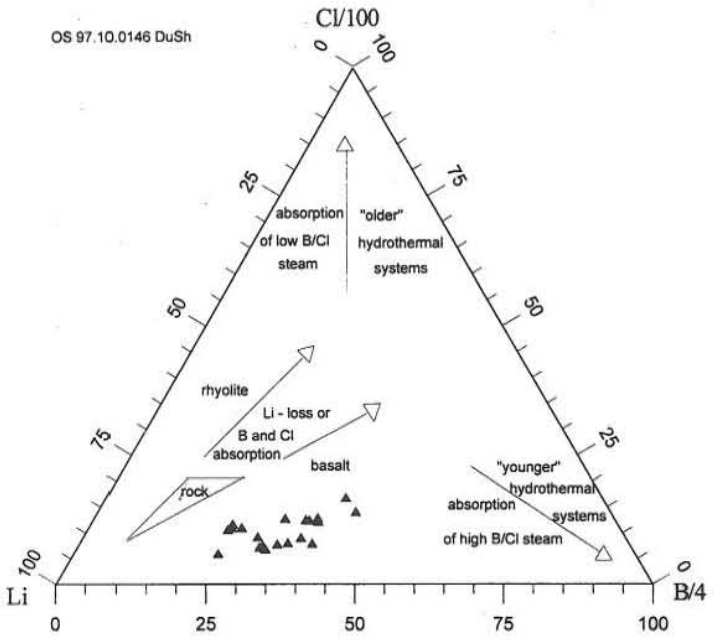

FIGURE 9: Cl-Li-B diagram for the Yangyi waters

4.3 Cl-SO_4-HCO_3 diagram

This diagram is used for the classification of thermal water based

TABLE 2: pH, Cl and B concentrations and mass ratios for the Yangyi waters

No.	Source	T (°C)	pH	Cl (ppm)	B (ppm)	Cl/B
1	ZK200	70	7.59	159	19.678	8.08
2	ZK203	61	7.97	160.8	18.67	8.61
3	ZK204	72	8.22	194.58	18.67	10.42
4	ZK206	21	7.2	166.64	18.92	8.81
5	ZK207	83	8.1	171.64	29.75	5.77
6	ZK208	86	8.49	180.58	33.02	5.47
7	ZK301	79	8.58	177.24	14.38	12.33
8	ZK302	77	7.76	157.97	19.42	8.13
9	ZK401	79	8.54	160.29	15.99	10.02
10	ZK402	65	8.86	150.4	17.48	8.60
11	ZK501	77	8.1	173.39	16.15	10.74
12	CHK4	34	8.35	80.91	7.06	11.46
13	Q4	86	9.4	181.55	29.895	6.07
14	Q5	83	9	167.85	28.419	5.91
15	Q6	84	8.86	68.51	13.472	5.09
16	Q7	57	8.7	188.4	30.374	6.20
17	Q8	78	5.69	4.45	4.54	0.98
18	Q206	77	8.01	77.06	6.81	11.32
19	Q405	74	9.68	161.23	20.43	7.89
20	Q408	82	6.2	3.55	2.31	1.54
21	Q502	50	8.5	151.67	25.85	5.87
22	Q572	50	7.6	83.19	13.43	6.19
24	river	13	7.3	1.71	1.22	1.40
25	river	14	7.43	1.71	1.59	1.08
26	river	6.5	7.49	12.01	1.11	10.82
27	river	7	7.97	20.19	1.48	13.64

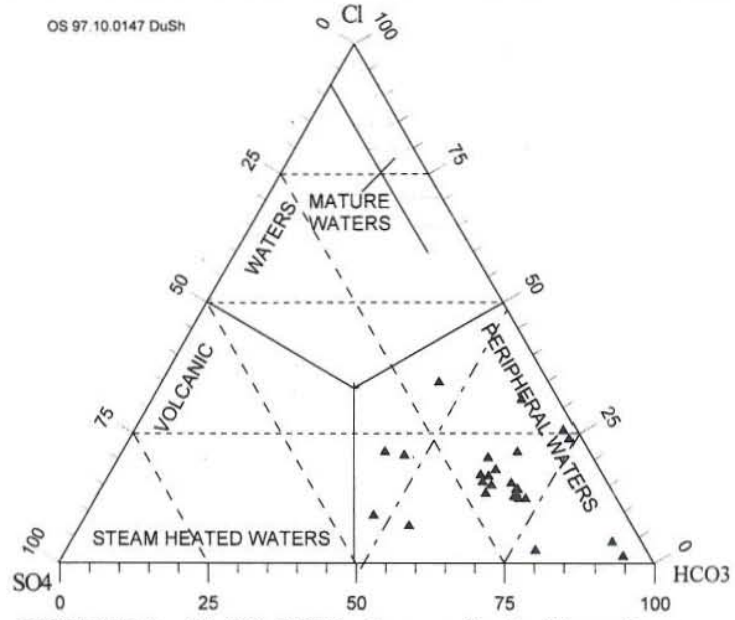

FIGURE 10: Cl-SO_4-HCO_3 diagram for the Yangyi waters

on three major anions Cl^-, SO_4^{-2} and HCO_3^-. In this diagram, compositional ranges are indicated for several typical groups of thermal waters such as volcanic and steam-heated waters, mature waters and peripheral waters. This diagram may provide an initial indication of mixing relationships or geographic groupings. For instance, Cl- water forms a central core, grading into HCO3- water toward the margins of a thermal area. High SO_4^{-2} steam-heated waters are usually encountered over the more elevated parts of a field. The degree of separation between data points for high chloride and bicarbonate waters may give an idea of the relative degree of interaction of the CO_2 charge fluid at lower temperature, and of the HCO_3^- concentration increased with time and distance travelled underground.

In this diagram, the data points for Yangyi waters plotted in the area of peripheral water (Figure 10) with about 75% HCO_3^- content. This area can be classed as a CO_2-rich discharge area.

Carbon-dioxide (CO_2)-rich waters have long been of interest. Barnes et al. (1978) pointed out that CO_2 is thought generally to come from three different sources, organic material, metamorphism of marine carbonate rocks, and the mantle. Stable isotope data are helpful in identifying the source of CO_2, especially where there is no evident near-surface source. The most

direct evidence for the isotope composition of CO_2 from mantle sources is provided by inclusions in volcanic rocks erupted along a spreading ridge. Barnes et al. (1978) also concluded that the ^{13}C isotope composition of mantle-derived CO_2 is evidently in or near the range of -4.7 to -8.0‰. Analytical data on ^{13}C for some well waters in the Yangyi field are in the range of -2.95‰ to -5.49, which suggests a mantle origin for CO_2.

Earthquakes are frequent in the Golug-Yangbajing-Nyemo geothermal active zone. There are records of 19 earthquakes of magnitude greater than 4.5 from 1921 to 1976, the largest being the 1951 Damxung-Chayu earthquake (Magn. 8.4). The latest earthquake took place near Yangbajing (Magn. 5.2) in 1992. The early phases are locally overlain by extended travertine layers in the Yangyi field. Carbonatic remains of former ascent channels of CO_2-rich waters can be localized. These tectonic fractures and the travertine are indications of periods of increased tectonic and seismic activity with cooled underground temperatures. Seismically active zones are often associated with major CO_2-outputs (Barnes et al., 1978).

Thus, the carbon dioxide could either be transported directly from the mantle as a separate gas phase or it could be expelled from cooling intrusions at depth. Carbon dioxide and liquid water will have different relative permeabilities. This could hinder mixing of the two phases and lead to the migration of a separate carbon dioxide phase along faults towards the surface; dissolution could take place at different depths or at the surface, producing thermal carbon dioxide water. If mixing occurs at a very high temperature, it is expected that equilibria with calcite and other minerals will be attained and fix the concentration of carbon dioxide in the water at a particular temperature (Arnórsson, 1979). This could be the explanation as to why carbon dioxide water dominates in the Yangyi geothermal field.

5. EVALUATION OF SUBSURFACE TEMPERATURE

5.1 Solute geothermometers

Various chemical geothermometers have been developed to predict reservoir temperature in geothermal systems, such as silica geothermometers (e.g Fournier and Rowe, 1966; Arnórsson, 1975; Fournier and Potter, 1982; Arnórsson et al., 1983a; Arnórsson, 1985), Na-K geothermometers (e.g. Fournier, 1979; Arnórsson et al., 1983a; Arnórsson, 1985; Giggenbach et al., 1983), and the Na-K-Ca geothermometer (Fournier and Truesdell, 1973; Arnórsson, 1985). These geothermometers are all based on the assumption that specific temperature dependent mineral/solute equilibria are attained in the geothermal reservoir.

When applied to the same field, the various geothermometers frequently yield appreciably different values for reservoir temperature. This may be due to a lack of equilibration between the respective solutes and hydrothermal minerals or due to reaction or mixing with cold water in the upflow; both processes modify the hot water composition. It is clearly desirable to have an approach that maximizes the use of the available analytical data for the water and allows the validity of the assumption of specific solution/mineral equilibria to be tested.

5.1.1 Silica geothermometers

The silica geothermometers are based on the solubility of different silica species such as quartz, chalcedony, cristobalite, or amorphous silica, and are widely used to estimate subsurface temperature in geothermal systems.

The quartz geothermometer is based on experimentally determined solubilities of quartz. The solubility of quartz appears to control dissolved silica in geothermal reservoirs at temperatures above 120-180°C. The quartz geothermometer presented by Fournier and Rowe (1966) could be used in the range 120-330°C with the following assumptions: The fluid is in equilibrium with quartz in the reservoir, the pore-fluid pressure in the reservoir is fixed by the vapour pressure of pure water (coexisting liquid and steam), there is no mixing of hotter and colder waters during upflow, and there is either conductive cooling of the ascending water or adiabatic cooling with steam separation at 100°C; Fournier (1973) presented the quartz geothermometer as the silica concentration with maximum steam loss at 100°C (SiO_2 is in mg/kg):

$$t(°C) = \frac{1522}{5.75 - logSiO_2} - 273.15 \quad (1)$$

The chalcedony geothermometer is based on the solubility of chalcedony. Fournier (1991) pointed out that there is an ambiguity in the use of silica geothermometers at temperatures below 180°C as chalcedony appears to control dissolved silica in some places and quartz in others. Chalcedony is a very fine-grained variety of quartz, which is probably not a separate mineral but a mixture of quartz and moganite (Gíslason et al., 1997) and with time it probably all changes to quartz. Temperature, time and fluid composition all affect different crystalline forms of silica. Thus, in some places (old systems) where water has been in contact with rock at a given temperature for a relative by long time, quartz may control dissolved silica at temperatures down to 100°C. In other places (young systems), chalcedony may control dissolved silica, at temperatures up to 180°C. The chalcedony geothermometer at the condition of maximum steam loss presented by Arnórsson et al. (1983a) is:

$$t(°C) = \frac{1264}{5.31 - logSiO_2} - 273.15 \quad (2)$$

As mentioned before, the chemical composition of the thermal fluid in the Yangyi geothermal system is mainly controlled by the reaction with host rock at temperatures between 170 and 210°C. Quartz and chalcedony may control the solubility of silica. Results of calculations for well discharges are listed in Table 3. The quartz geothermometer temperatures are in the range 144-220°C and the chalcedony temperatures 121-207°C. The quartz geothermometer gives 25°C higher temperatures than the measured downhole temperatures for most samples, but the chalcedony geothermometer gives approximately the same values as measured temperatures. For some wells, for instance samples ZK200 and ZK208, the chalcedony geothermometer gives the same values as those measured, i.e. 172°C and 207°C, respectively.

5.1.2 Cation geothermometers

The Na-K geothermometer is based on the exchange of Na^+ and K^+ ions between coexisting alkali feldspars with temperature-dependent equilibrium constants:

$$NaAlSi_3O_8 + K^+ = KAlSi_3O_8 + Na^+ \quad (3)$$

The equilibrium constant, K_{eq}, for Reaction 3 is

TABLE 3: Results for different geothermometers for the Yangyi waters

No.	Source	t_{meas}	t_1	t_2	t_6	t_7	t_8	t_9
1	ZK200	172	191	172	193	210	127	183
2	ZK203	203	189	170	191	208	166	177
3	ZK204	144	171	150	173	191	154	174
4	ZK206	152	171	150	183	200		177
5	ZK207	163	176	156	95	116	73	112
6	ZK208	207	222	207	217	232	109	227
7	ZK301	165	192	174	208	224	132	198
8	ZK302	130	161	139	168	186	124	166
9	ZK401	136	166	145	184	202	128	177
10	ZK402	104	144	121	107	128	93	121
11	ZK501	141	191	172	189	206	144	187
12	CHK4		153	131	210	226	79	171

t_1 = Quartz temp. (Fournier, 1973); t_2 = Chalcedony temp. (Arnórsson et al., 1983a);
t_6 = Na-K temp. (Fournier, 1979); t_7 = Na-K temp. (Giggenbach, 1988);
t_8 = K-Mg temp. (Giggenbach, 1988); t_9 = Na-K-Mg temp. (Fournier and Truesdell, 1973);
t_{meas} = Measured temperature at main feed zone

$$K_{eq} = \frac{[KAlSi_3O_8]\,[Na^+]}{[NaAlSi_3O_8]\,[K^+]} \tag{4}$$

In the application of Equation 4, the usual simplifying assumptions are that the activities of the solid reactants are unity and the activities of the dissolved species about equal to their molal concentration in aqueous solution. Thus, Equation 4 reduces to

$$K_{eq} = \frac{[Na^+]}{[K^+]} \tag{5}$$

Many temperature functions have been presented for the Na-K geothermometers by various authors, but there is a large discrepancy between temperatures resulting from the different equations. The following formulae are used in this report (the concentration of Na and K are in mg/kg):

Na/K temperature (Fournier, 1979)

$$t(°C) = \frac{1217}{1.483 + \log(Na/K)} - 273{,}15 \tag{6}$$

Na/K temperature (Giggenbach 1988)

$$t(°C) = \frac{1390}{1.75 + \log(Na/K)} - 273.15 \quad (7)$$

The K-Mg geothermometer (Giggenbach, 1988), based on the equilibrium between water and the mineral assemblage K-feldspar, K-mica and chlorite, is found to respond fast to changes in the physical environment and usually gives a relatively low temperature. This geothermometer is also reasonable for estimation of reservoir temperature (concentrations are in mg/kg):

$$t(°C) = \frac{4410}{14.0 - \log(K^2/Mg)} - 273.15 \quad (8)$$

The Na-K-Ca geothermometer (Fournier and Truesdell, 1973) takes into account a reaction involving the exchange of Na+, K+ and Ca+ with a mineral solid solution. This minimizes but does not eliminate effects of disregarding the activity coefficients of solids. The geothermometer is entirely empirical and assumes a base exchange reaction at temperatures above approximately 100°C and below approximately 100°C (concentration are in mg/kg)

$$t(°C) = \frac{1647}{logNa/K + \beta\,[\log(\sqrt{Ca}/Na) + 2.06] + 2.47} - 273.15 \quad (9)$$

1) Calculate $[\log(Ca^{1/2}/Na)+2.06]$; if it is positive, calculate the temperature, t, using $\beta=4/3$.
2) If $t<100°C$, use this temperature.
3) If $t>100°C$ or $[\log(Ca^{1/2}/Na)+2.06]$ is negative, then use $\beta=1/3$ to calculate the temperature.

Table 3 shows the results for different cation geothermometers. The results for most of the samples are in the range 186-220°C for Na/K temperature (Giggenbach, 1988) and 168-217°C for Na/K temperature (Fournier, 1979). Samples ZK207 and ZK402 give the lowest Na/K temperatures probably, due to analytical error for the ion K^+. The Na/K geothermometer (Fournier, 1979) differs by 3 to 48°C.

The Na-K-Ca geothermometer, using $\beta=1/3$, yields higher than measured temperatures in the range 112-227°C. Comparison of silica and cation geothermometer results shows that chalcedony and Fournier's (1979) Na-K geothermometers give approximately similar results and seem to be the best suited geothermometers for the Yangyi thermal waters. The Na-K temperatures are equal to or higher than the chalcedony equilibrium temperatures (Figure 11).

5.2 Na-K-Mg diagram

Giggenbach (1988) presented a triangular diagram, in terms of Na/1000, K/100 and Mg which is based on the temperature of two sub-systems, K-Na and K-Mg, according to

$$L_{kn} = \log(C_K/C_{Na}) = 1.75 - 1390/T \quad (10)$$

$$L_{km} = \log(C_K^2/C_{Mg}) = 14.0 - 4410/T \quad (11)$$

The internally consistent temperature dependence of the quotient C^2_{Na+}/C_{Mg2+} is simply obtained by use of

$$L_{nm} = L_{km} - 2L_{Kn} = \log(C_{Na}^2/C_{Mg}) = 10.5 - 1630/T \quad (12)$$

In a fully equilibrated system each of the three relationships above is equally valid. Of the two sub-systems, K-Na is most likely to provide the basis for a suitable geothermometer. Two sets of isotherms are presented in a Na-K-Mg triangular diagram. Their intersections correspond to the composition of water in equilibrium with both mineral systems, resulting in the "full equilibrium" curve. Thus, evaluation of analytical Na, K and Mg concentrations by use of this diagram allows a clear distinction to be made between waters suitable or unsuitable for the application of ionic solute geothermometers. Deeper equilibration temperatures and the effects of processes such as re-equilibrium and mixing of waters of different origins can, thus, be assessed simultaneously for a large number of samples.

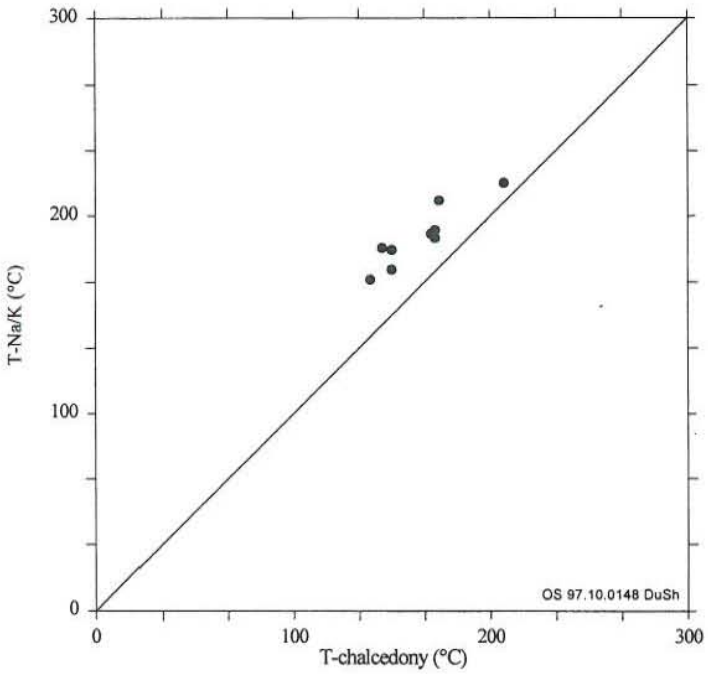

FIGURE 11: Relationship between the chalcedony equilibrium temperature and the Na-K temperature

The Na-K-Mg triangular diagram is shown in Figure 12. The data points on the diagram plot mainly in three groups: 1) Samples 1, 5, 7, 8, 9 and 11 plot below the equilibrium curve of Arnórsson et al. (1983a) and are partially equilibrated waters; this is probably due to mixing of the thermal water with local cold groundwater. 2) Samples 2, 3 and 10 plot a little above the equilibrium curve. This might be caused by steam

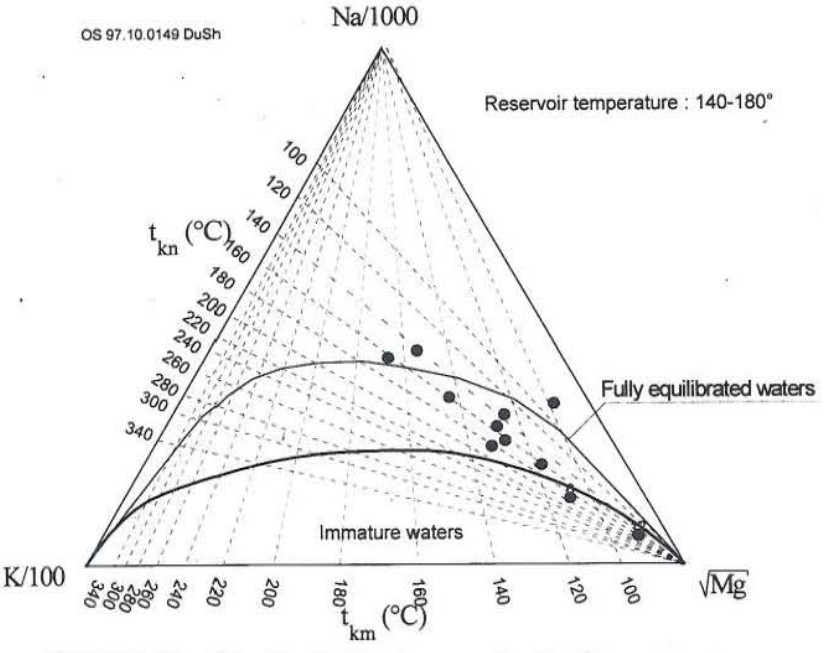

FIGURE 12: The Na-K-Mg diagram for the Yangyi waters

loss which would increase the absolute solute concentrations of samples. 3) Samples 6 and 12 plot in the "immature" area, indicating that these waters are unsuitable for the evaluation of Na/K equilibration temperature. Applying the diagram to Yangyi waters indicates that most well samples are partially equilibrated waters with the reservoir temperature T_{kn} in the range 140-180°C and T_{km} 120-180°C.

5.3 Solution-mineral equilibria

As mentioned before, when applied to the same field, the various geothermometers frequently yield appreciably different values for reservoir temperature. Reed and Spycher (1984) have proposed that the best estimate of reservoir temperature can be attained by considering, simultaneously, the state of equilibrium between a specific water and many hydrothermal minerals as a function of temperature. They pointed out that if a group of minerals approaches equilibrium at a particular temperature, this temperature corresponds to the most likely reservoir temperature, or at least the source aquifer temperature of the particular water considered.

The calculations were performed using the WATCH aqueous speciation program of Arnórsson et al. (1982) and Bjarnason (1994) to construct the mineral equilibrium diagram (Figure 13), showing the saturation index, log(Q/K), from 25 to 200°C for Samples 1-12 in the Yangyi field.

The concentration of Al was only determined in sample Q408, and a gas sample was only collected for sample ZK200. The analytical result, for both Al and gas concentrations for these two samples have been assumed for all well samples for the construction of mineral equilibrium diagrams.

It can be seen from these diagrams, that at a certain temperature there is no clear water-rock equilibrium attained between all the minerals and thermal fluid. Chalcedony equilibrated with thermal fluid at temperatures in the range 150-175°C. The best equilibrium temperature for sample ZK200 was in good agreement with the measured temperature. For this sample, the chalcedony-equilibrium temperature of 170°C deviated only 2°C from the measured temperature of 172°C. The calculated temperatures are lower than measured temperatures for samples ZK203 and ZK208. These diagrams also show that most minerals appear to reach equilibrium in the temperature range 80-120°C.

6. MIXING MODELS

Geothermal water which ascends from a reservoir and emerges at the surface in hot springs may cool on the way, by conduction, boiling or mixing with shallow cold water, or by any combination of these three processes as suggested by Arnórsson (1985). The chemical composition of this water in surface discharge may be used to evaluate underground temperature. Samples of well discharges have also been used in the present study for comparison.

6.1 Evidence of mixing

According to the previous discussion, there is some evidence to infer processes of mixing in the thermal water at Yangyi. Firstly, on the Na-K-Mg triangular diagram (Figure 12), most samples, particularly spring samples, plot in the partial equilibrium area. Secondly, mineral-solution diagrams show no clear equilibrium between thermal water and any group of minerals. Thirdly, a linear relationship between Cl and most of the constituents is observed for samples from the Yangyi field (Figure 14). Arnórsson (1985) suggests that such behaviour is evidence of mixing.

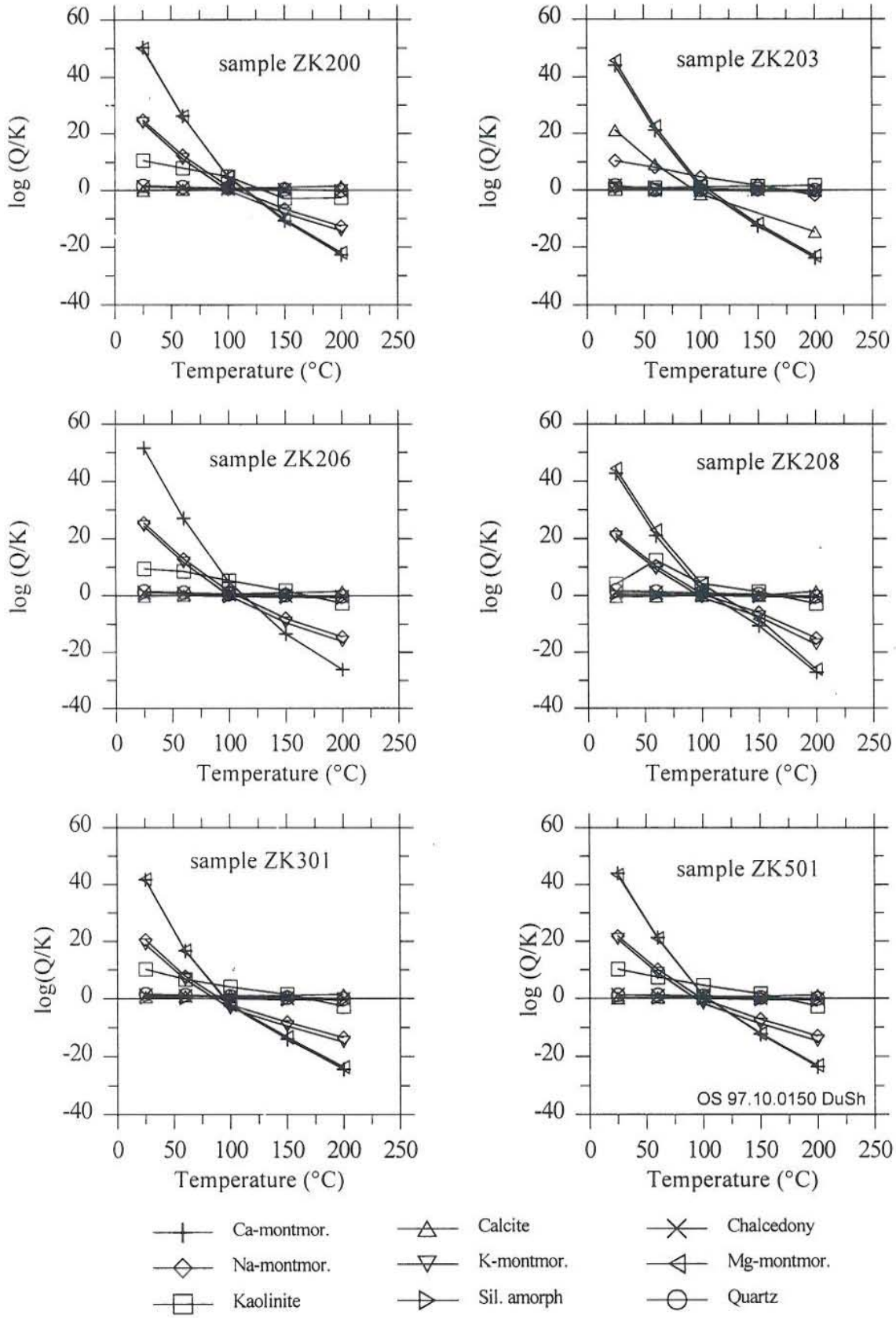

FIGURE 13: Saturation index (log Q/K) vs. temperature for Yangyi waters calculated with WATCH

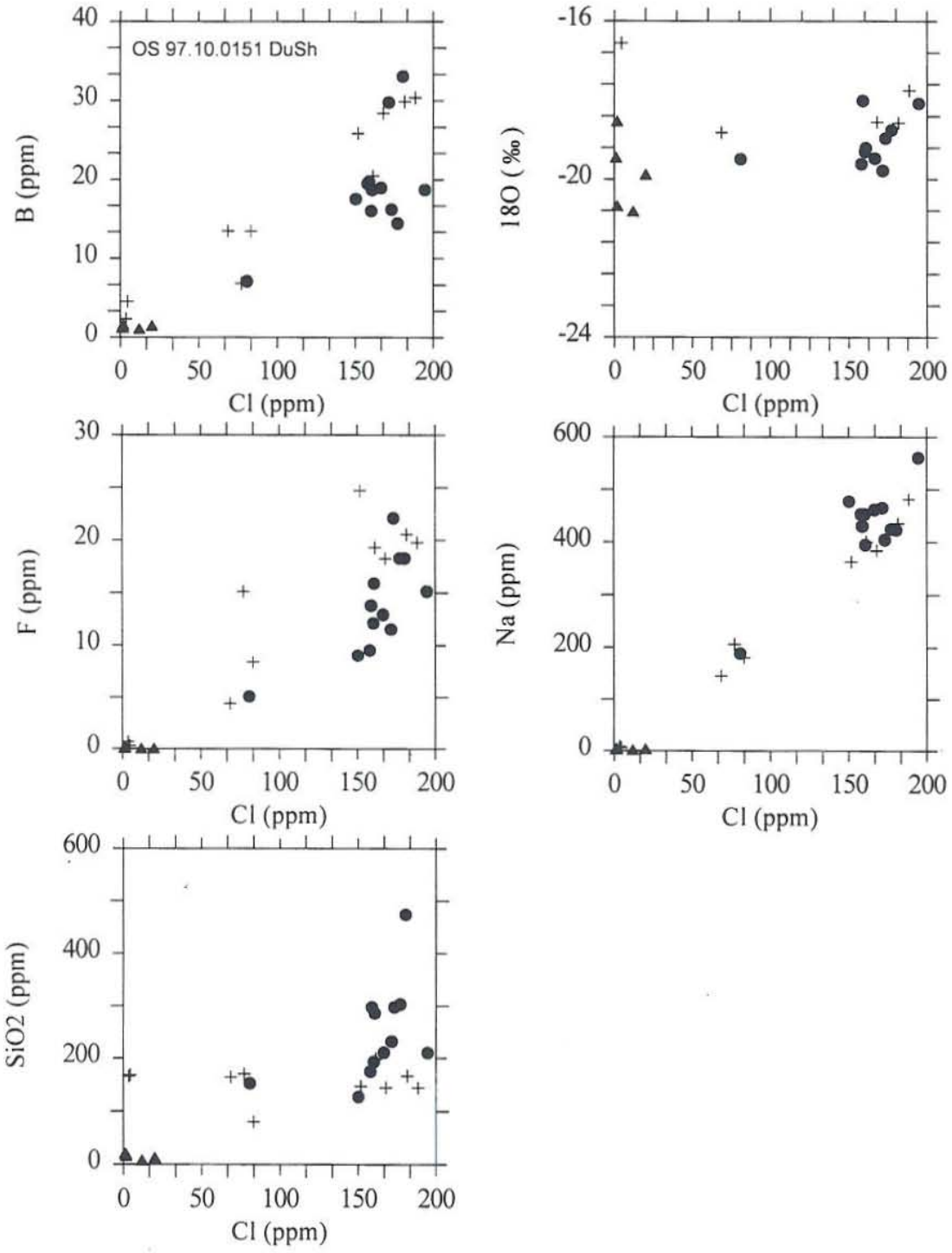

FIGURE 14: Relationship between Cl and some other constituents in Yangyi waters

There are some differences between the linear relations of Cl to other constituents in well discharges and spring waters. These indicate strong mixing in spring waters ascending to the surface, while water with an approximately constant Cl concentration discharging from wells, suggests conductive cooling. Thus, casing prevents the entrance of cold water.

6.2 Silica-enthalpy mixing model

The water in many hot springs consists of mixtures of deep hot water and shallow cold water. Truesdell and Fournier (1977) have proposed a plot of dissolved silica versus enthalpy of the spring water to estimate the temperature of the deep hot water component.

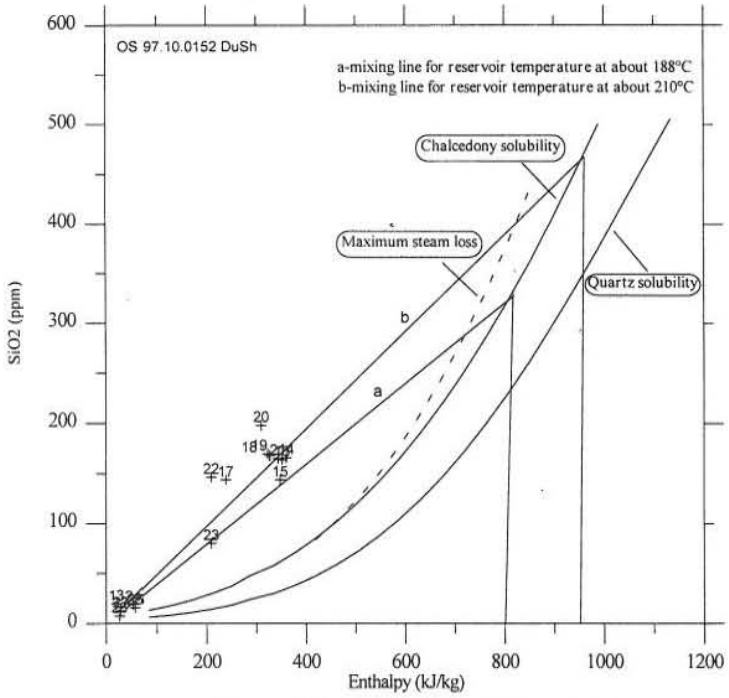

FIGURE 15: Silica-enthalpy mixing model for the Yangyi waters

Figure 15 shows the silica-enthalpy mixing model as applied to the Yangyi geothermal system. There, chalcedony is expected to control the silica solubility of the thermal water. Two mixing lines have been plotted. Mixing line-a connects cold water sample Q2 , a sample of local stream water, and hot spring samples Q572 and Q5 to intersect the chalcedony solubility curve at the enthalpy value of about 800 kJ/kg, which corresponds to an original temperature of 188°C for the hot water component. Mixing line-b, which connects samples of cold waters and hot spring samples Q4, Q6, Q8, Q206 and Q408, intersects the chalcedony solubility curve at an enthalpy value of about 920 kJ/kg which corresponds to 210°C reservoir temperature. The silica concentrations of samples Q7 and Q405 are higher, probably due to boiling.

6.3 Enthalpy-chloride mixing model

Fournier (1977) suggested the use of an enthalpy-chloride diagram to predict underground temperature. This mixing model takes into account both mixing and boiling processes. Its application basically involves relating analysed chloride levels to water enthalpy which can be derived from measured discharge temperature, geothermometry temperature, and silica-enthalpy mixing model temperature.

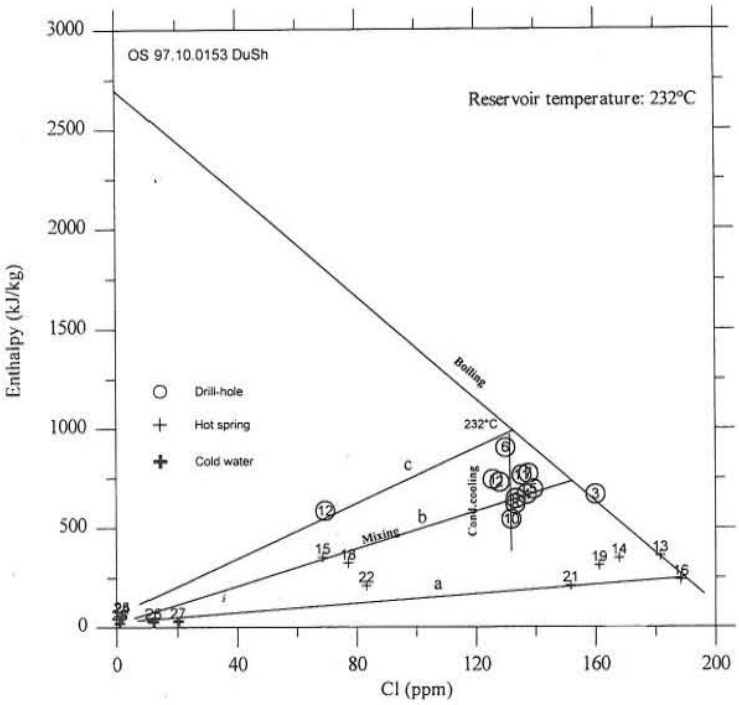

FIGURE 16: Enthalpy-chloride mixing model for the Yangyi waters

The enthalpy-chloride mixing model for the Yangyi waters is shown in Figure 16. In this diagram, most of the spring waters lie along the mixing line. Line a connects samples 13, 14,

16, 19, 21 and cold water samples 24, 25, 26, and 27. The former are probably cooled by two processes, the ascending deep hot water boiled and then mixed with cold water at shallow depth. Line b connects well water samples and hot spring samples 15, 18 with cold waters. This result suggests that ascending waters cooled further by conduction before mixing. Line c connects well samples 6, 12 and cold waters, and it seems that the dominating process for cooling well waters is mixing with cold water. The boiling line connects samples 3, 13 and 16, and thus suggests ascending water cooled by boiling with loss of steam, forming the highest Cl water (sample 16).

The enthalpy-chloride mixing model suggests that thermal water can be found at different depths, representing mixed water of different origins and different temperatures. It has been indicated by this model that the hot end member, tapped by drilling, at present has a minimum temperature of 207°C, and that hot unmixed water with temperatures of about 232°C probably exists deep down in the reservoir.

6.4 Silica-carbonate mixing model

Arnórsson et al. (1983b) found that the concentration of carbon dioxide in geothermal reservoir waters was only dependent on the temperature of these waters. At a temperature of about 200°C, most of the dissolved total carbonate is in the form of carbon dioxide, so it is a satisfactory approximation to take analysed carbonate to represent carbon dioxide. The silica concentration in high-temperature water is determined by quartz solubility. Thus, it is a satisfactory approximation to assume a fixed relationship between silica and total carbonate in a high-temperature geothermal reservoir. Boiling of such water will lead to a drastic reduction in its carbonate content but mixing without boiling will, on the other hand, produce waters with high carbonate/silica ratios relative to equilibrated water.

The silica-carbonate diagram may be used to aid geothermometry interpretation. First, it serves to distinguish boiled water from conductively cooled water; mixed waters contain an underground hot water component, assuming that boiling occurs between the points of last equilibrium with quartz and sampling. Secondly, if there is sufficient data on warm waters containing an unboiled water component, the diagram may be used to evaluate the temperature of the hot water component.

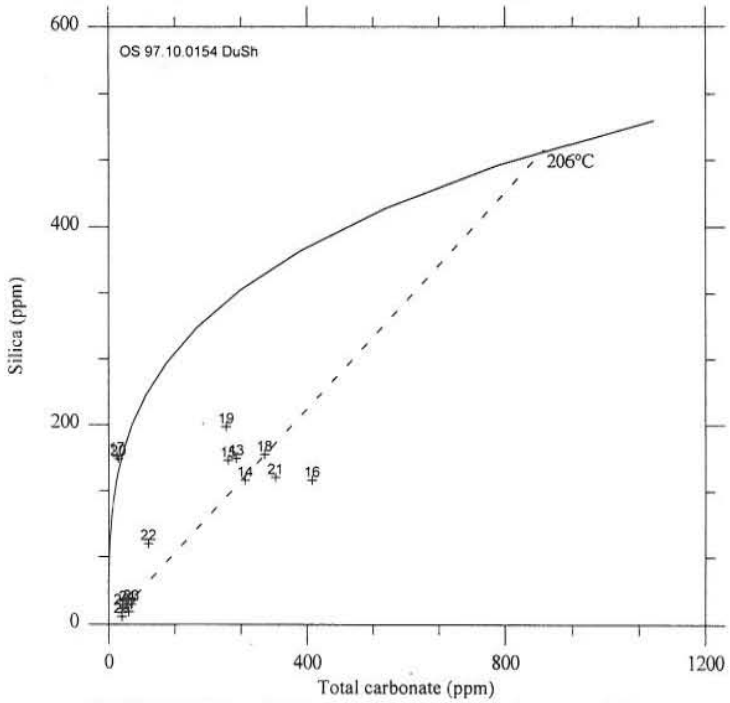

FIGURE 17: Silica-carbonate mixing model for the Yangyi waters

Estimation of underground temperature by the silica-carbonate mixing model involves the extrapolation of a line through the data points for mixed and undegassed waters and a demonstration of the intersection points with a silica-carbonate curve of equilibrated waters. The quartz geothermometer is used to obtain the temperature from the silica concentration corresponding to this point.

In the Yangyi geothermal field a linear relationship between silica and carbonate is observed for most of the cold and warm waters (Figure 17), indicating that the hot water component of the mixed water has

not boiled. An extrapolation of a line through the data points indicates that the hot water component is at about 206°C. Two water samples (17, 20) contain relatively little carbonate. This low concentration of carbonate might be due to near-surface boiling with CO_2 loss before sampling. These samples also have a low Cl content (4.45 ppm and 3.55 ppm) and the isotope ratio for sample 17 is similar to those of the local meteoric water, which suggests that this water is probably formed by steam heating of the shallow cold water.

7. CONCLUSIONS

The main purpose of this report was to predict the subsurface temperatures for the Yangyi geothermal field using the chemical composition of hot spring water, and compare it to measured temperatures in boreholes drilled from 1986 to 1990. Furthermore, some understanding of the chemical processes taking place within the geothermal system has been obtained by this. The following are the main conclusions of this study:

1. Hydrogen and oxygen isotope ratios suggest local meteoric origin for the thermal fluid, which has taken part in a long-term deep circulation and interaction with host rock as suggested by a significant oxygen-shift.

2. Mixing and conductive cooling are the main processes controlling the chemical composition of thermal fluids in the Yangyi geothermal system.

3. Carbon dioxide could either be transported directly from the mantle as a separate gas phase or it could be expelled from cooling intrusions at depth. Dissolution of carbon dioxide could take place at different depths or at the surface, producing the thermal carbon dioxide waters which predominate in the Yangyi geothermal system.

4. Solution-mineral diagrams suggest that chalcedony probably controls the solubility of silica. The quartz geothermometer suggests a subsurface temperature ranging from 140°C to 220°C. Mixing models suggest a subsurface temperature of 188-232°C in the deep part of the geothermal system.

ACKNOWLEDGEMENTS

I would like to express my gratitude to Dr. Ingvar Birgir Fridleifsson for his selection of myself to attend the UNU Geothermal Training Programme, and for his guidance and advice throughout the whole training period. My thanks are due to Dr. Halldór Ármannsson, my advisor, for sharing his experience and critical advice during all stages of preparing this report. Special thanks go to Ludvik S. Georgsson and Gudrún Bjarnadóttir for their assistance and arrangement in the past six months during the training programme and my stay in Iceland.

My thanks go to all the lecturers and staff members at Orkustofnun, for their comprehensive presentations and willingness to share their knowledge and experience, especially in geochemistry. I also thank my co-Fellow from El Salvador, Marbin Antonio Martínez Flores, for discussions and suggestions during the writing of this report.

Finally, I express my thanks to the Directors of the Bureau of Geology and Mineral Resources of Tibet and the Geothermal Geological Team of Tibet for supporting me in attending this training programme.

REFERENCES

Árnason, B.,1976: *Groundwater systems in Iceland traced by deuterium.* Soc. Sci. Islandica, 42, Reykjavík, 236 pp.

Arnórsson, S., 1975: Application of the silica geothermometer in low-temperature hydrothermal areas in Iceland. *Am. J. of Sci.,* 275, 763-783.

Arnórsson, S., 1979: Mineral deposition from Icelandic geothermal waters: Environmental and utilization problems. *Proceedings of the SPE International Symposium on Oilfield and Geothermal Chemistry, Houston, Texas,* 267-274.

Arnórsson, S., 1985: The use of mixing models and chemical geothermometers for estimating underground temperature in geothermal systems. *J. Volc. Geotherm. Res., 23,* 299-335.

Arnórsson, S., Gunnlaugsson, E. and Svavarsson, H., 1983a: The chemistry of geothermal waters in Iceland. III. Chemical geothermometry in geothermal investigations. *Geochim. Cosmochim. Acta, 47,* 567-577.

Arnórsson, S., Gunnlaugsson, E., and Svavarsson, H., 1983b: The chemistry of geothermal waters in Iceland. II. Mineral equilibria and independent variables controlling water compositions. *Geochim. Cosmochim. Acta, 47,* 547-566.

Arnórsson, S., Sigurdsson, S., and Svavarsson, H., 1982: The chemistry of geothermal waters in Iceland I. Calculation of aqueous speciation from 0°C to 370°C. *Geochem. Cosmochim. Acta, 46,* 1513-1532.

Barnes, I., Irwin, W.P. and White, D.E. 1978: *Global distribution of carbon dioxide discharges and major zones of seismicity.* U.S. Geological Survey, Water Resources Investigations, 78-39, report, 12 pp.

Bjarnason; J.Ö., 1994: *The speciation program WATCH, version 2.1.* Orkustofnun, Reykjavík, 7 pp.

Fournier, R.O., 1973: Silica in thermal waters. Laboratory and field investigations. *Proceedings of the International Symposium on Hydrogeochemistry and Biochemistry, Tokyo, 1, Clark Co., Washington D.C.,* 122-139.

Fournier, R.O., 1977: Chemical geothermometers and mixing model for geothermal systems. *Geothermics, 5,* 41-50.

Fournier, R.O., 1979: A revised equation for the Na-K geothermometer. *Geoth. Res. Council, Transactions, 3,* 221-224.

Fournier, R.O., 1991: Water geothermometers applied to geothermal energy. In: D'Amore, F. (coordinator), *Application of Geochemistry in Geothermal Reservoir Development.* UNITAR/UNDP publication, Rome, 37-69.

Fournier, R.O., and Potter, R.W. II., 1982: A revised and expanded silica (quartz) geothermometer. *Geoth. Res. Council, Bull., 11-10,* 3-12.

Fournier, R.O., and Rowe, J.J., 1966: Estimation of underground temperatures from the silica content of water from hot springs and wet steam wells. *Am. J. Sci., 264,* 685-697.

Fournier, R.O., and Truesdell, A.H., 1973: An empirical Na-K-Ca geothermometer for natural waters. *Geochim. Cosmochim. Acta, 37,* 1255-1275.

Giggenbach, W.F., 1988: Geothermal solute equilibria. Deviation of Na-K-Mg-Ca geoindicators. *Geochim. Cosmochim. Acta, 52,* 2749-2765.

Giggenbach, W.F., 1991: Chemical techniques in geothermal exploration. In: D'Amore, F. (coordinator), *Application of geochemistry in geothermal reservoir development,* UNITAR/UNDP publication, Rome, 119-142.

Giggenbach, W.F., 1992: Isotope shift in waters from geothermal and volcanic systems along convergent plate boundaries and their origin. *Earth and Planetary Sci. Lett., 113,* 495-510.

Giggenbach, W.F., Gonfiantini, R., Jangi, B.L, and Truesdell, A.H., 1983: Isotopic and chemical composition of Parbati Valley geothermal discharges, NW-Himalaya, India. *Geothermics, 12,* 199-222.

Gíslason, S.R., Heaney, P.J., Oelkers, E.H. and Schott, J. 1997: Kinetic and thermodynamic properties of moganite, a novel silica polymorph. *Geochim. Cosmochim. Acta, 61,* 1193-1204.

Liang T., 1992: Preliminary research on the exploration method at Yangyi geothermal field. In: *Reports of the International Workshop on the High-Temperature Geothermal Fields in Tibet,* 154-159.

Liang T. et al., 1990: *Exploration report of Yangyi geothermal field, Dangxong county, Tibet Autonomous Region.*

Qin Changlong, 1996: *Geothermal geology in Tibet.* Field trip guide T388 for the 30th International Geological Congress, Bejing, China, Geological Publ. House.

Reed, M.H., and Spycher, N.F., 1984: Calculation of pH and mineral equilibria in hydrothermal water with application to geothermometry and studies of boiling and dilution. *Geochim. Cosmochim. Acta, 48,* 1479-1490.

Truesdell, A.H., 1976: Summary of section III - geochemical techniques in exploration. *Proceedings of the 2nd U.N. Symposium on the Development and Use of Geothermal Resources, San Francisco, 1,* Iiii-Ixxix.

Truesdell, A.H., and Fournier, R.O., 1977: Procedure for estimating the temperature of a hot water component in a mixed water using a plot of dissolved silica vs. enthalpy. *U.S. Geol. Survey J. Res.,* 5, 49-52.

Zhu M., and Xu Y., 1992: Hydrothermal alteration and evaluation in the Yangyi geothermal field of Tibet, China. In: *Reports of The International Workshop on the High-Temperature Geothermal Fields in Tibet.,* 125-133.